ISSN 1063-7788, Physics of Atomic Nuclei, 2011, Vol. 74, No. 4, pp. 573–579. © Pleiades Publishing, Ltd., 2011.
Original Russian Text © Yu.E. Titarenko, V.F. Batyaev, A.Yu. Titarenko, M.A. Butko, K.V. Pavlov, S.N. Florya, R.S. Tikhonov, V.M. Zhivun, A.V. Ignatyuk, S.G. Mashnik, S. Leray, A. Boudard, J. Cugnon, D. Mancusi, Y. Yariv, K. Nishihara, N. Matsuda, H. Kumawat, G. Mank, W. Gudowski, 2011, published in Yadernaya Fizika, 2011, Vol. 74, No. 4, pp. 596–603.

NUCLEI
Experiment

Measurement and Simulation of the Cross Sections for the Production of ^{148}Gd in thin ^{nat}W and ^{181}Ta Targets Irradiated with 0.4- to 2.6-GeV Protons

Yu. E. Titarenko[1)*], V. F. Batyaev[1)], A. Yu. Titarenko[1)], M. A. Butko[1)], K. V. Pavlov[1)], S. N. Florya[1)], R. S. Tikhonov[1)], V. M. Zhivun[1)], A. V. Ignatyuk[2)], S. G. Mashnik[3)], S. Leray[4)], A. Boudard[4)], J. Cugnon[5)], D. Mancusi[5)], Y. Yariv[6)], K. Nishihara[7)], N. Matsuda[7)], H. Kumawat[8)], G. Mank[9)], and W. Gudowski[10)]

Received October 7, 2010

Abstract—The cross sections for the production of ^{148}Gd in ^{nat}W and ^{181}Ta targets irradiated by 0.4-, 0.6-, 0.8-, 1.2-, 1.6-, and 2.6-GeV protons at the ITEP accelerator complex have been measured by direct α spectrometry without chemical separation. The experimental data have been compared with the data obtained at other laboratories and with the theoretical simulations of the yields on the basis of the BERTINI, ISABEL, CEM03.02, INCL4.2, INCL4.5, CASCADE07, and PHITS codes.

DOI: 10.1134/S1063778811040193

INTRODUCTION

Over the last fifteen years, a cycle of studies devoted to determining the yields of radioactive residual nuclei in targets and structural materials of electronuclear facilities has been performed at ITEP [1–3]. The cross sections for nuclide production in those experiments were determined by my means of precision γ spectrometry using HPGe spectrometers. This approach ensures the determination of products having significant (usually above ~0.1%) yields of γ rays per decay event. However, some product radioactive nuclei are exclusively α and β emitters, which cannot be detected by HPGe spectrometers. At the same time, knowledge of their yields is very important for applications, because they can significantly contribute to the radiation hazard in processing and utilizing the elements of electronuclear facilities.

One of such important products is ^{148}Gd ($T_{1/2}$ = 74.6 yr), which is an α emitter accumulated in all heavy target materials irradiated with protons of energy above ~0.5 GeV. There is only one work [4] in which the yields of ^{148}Gd in ^{nat}W, ^{181}Ta, and ^{197}Au targets irradiated by 0.6- and 0.8-GeV protons were systematically measured. This amount of data is insufficient for applications, where the initial proton energy is usually not less than ~1 GeV. For this reason, the cross sections for the production of ^{148}Gd in thin ^{nat}W and ^{181}Ta targets were measured at ITEP for the proton energies of 0.4, 0.6, 0.8, 1.2, 1.6, and 2.6 GeV.

IRRADIATION AND MEASUREMENTS

The experimental samples were irradiated by an extracted proton beam of the ITEP accelerator complex. The main beam parameters were presented in [1–3]. The targets were assemblies of samples and monitors 10.5 mm in diameter. The weights of the ^{nat}W and ^{181}Ta samples, the sequences of the samples in the assemblies, the irradiation duration, and the proton fluence are presented in Table 1. The proton fluence was determined using the ^{27}Al$(p,x)^{22}$Na monitor reaction whose excitation function is well known [5].

The detection of α particles emitted by ^{148}Gd ($T_{1/2}$ = 74.6 yr, E_α = 3.183 MeV, η = 100%) was performed using an α spectrometer based on a

[1)]Institute for Theoretical and Experimental Physics, ul. Bol'shaya Cheremushkinskaya 25, Moscow, 117218 Russia.
[2)]Institute of Physics and Power Engineering, pl. Bondarenko 1, Obninsk, Kaluga oblast, 249033 Russia.
[3)]Los Alamos National Laboratory, USA.
[4)]CEA, Saclay, France.
[5)]University of Liege, Belgium.
[6)]Soreq NRC, Yavne, Israel.
[7)]JAEA, Tokai, Japan.
[8)]BARC, Mumbai, India.
[9)]IAEA, Vienna, Austria.
[10)]Royal Institute of Technology, Stockholm, Sweden.
[*]E-mail: Yury.Titarenko@itep.ru

Table 1. Main irradiation parameters

Proton energy, GeV	Irradiation date	Stack	Sample mass, g		$^{27}Al(p,x)^{22}Na$ cross section, mb	Average proton fluence, $p/(cm^2\ s) \times 10^{-10}$	
			^{nat}W	^{181}Ta		^{nat}W	^{181}Ta
0.4	October 18–19, 2007	Ta–Al–W–Al	0.276	0.353	15.8 ± 1.0	1.79 ± 0.15	1.89 ± 0.16
0.6	October 15–16, 2007	Ta–Al–W–Al	0.267	0.3555	16.0 ± 1.0	7.82 ± 0.56	7.97 ± 0.57
0.8	June 22–25, 2007	W–Al–Ta–Al	0.2590	0.3584	15.5 ± 1.0	8.05 ± 0.60	8.55 ± 0.64
1.2	June 20–2, 2007	W–Al–Ta–Al	0.269	0.355	14.4 ± 1.0	5.00 ± 0.36	5.12 ± 0.37
1.6	March 28–3 April, 2006	W–Al–Ta–Al	0.0328	0.1236	13.2 ± 1.0	6.24 ± 0.51	5.65 ± 0.57
2.6	November 27, 2006	W–Al–Ta–Al	0.2566	0.3598	11.4 ± 0.9	6.91 ± 0.62	7.44 ± 0.65

Table 2. Detection efficiency of the α spectrometer

Distance from the source to the detector, mm	Detection efficiency		
	measured using ^{239}Pu	calculated with AASI	calculated with MCNPX
4	0.294 ± 0.018	0.2942 ± 0.0015	0.29485 ± 0.00015

Si detector (with a resolution of 17 keV for the 5275.3-keV α ^{243}Am line for a vacuum of ~250 μm Hg in a measurement chamber) and a 2048-channel emulator–analyzer board of an IBM PC. The α spectrometer was calibrated using a set of standard α sources ^{239}Pu, ^{238}Pu, ^{226}Ra, and ^{233}U. Figure 1 shows one of the measured calibration spectra. After the calibration measurements, the background of the α chamber was measured; the results are presented in Fig. 2. Figure 3 shows the measured energy calibration. Figure 4 shows the detection efficiency of the spectrometer, obtained using ^{239}Pu (5156.6 keV), as a function of the distance between the source and the surface of the detector, measured without a collimator. The measured detection efficiency is in good agreement with the calculated value obtained by the AASI code for the simulation of the energy spectrum in the α spectrometer [6]. This quantity was also calculated using the MCNPX code, where the real sample–detector geometry was specified and 3183-keV α particles were taken with isotropic angular and uniform spatial distributions throughout the volume of each experimental sample. The detection efficiencies for a distance of 4 mm between the source and the surface of the detector used in the measurements are presented in Table 2.

Table 3. Cross section for the production of ^{148}Gd (in millibarns) in ^{181}Ta and ^{nat}W targets

Proton energy, GeV	^{181}Ta		^{nat}W	
	this work	[4]	this work	[4]
0.4	2.11 ± 0.28		1.04 ± 0.15	
0.6	14.8 ± 2.3	15.2 ± 4.0	8.78 ± 1.08	8.31 ± 0.92
0.8	22.3 ± 2.8	28.6 ± 3.5	21 ± 3	19.4 ± 1.8
1.2	27.7 ± 3.4		25.7 ± 3.2	
1.6	31.7 ± 4.8		26.7 ± 3.4	
2.6	21.4 ± 3.2		16.8 ± 2.9	

One of the measured α spectra of the irradiated ^{nat}W and ^{181}Ta samples is shown in Fig. 5. It can be seen that these spectra are significantly different from the spectra of the standard "thin" α sources in Fig. 1. This difference is caused by the deceleration of 3183-keV α particles emitted by ^{148}Gd in the material of the sample; this leads to the complete spread of the ^{148}Gd monoline and the detection of α particles having energies from 3183 keV to the lower discrimination energy of the spectrometer (~80 keV). In view of the presence of a large amount of β-active nuclei in the irradiated samples, the spectrometer also detects their total spectrum. The difference between

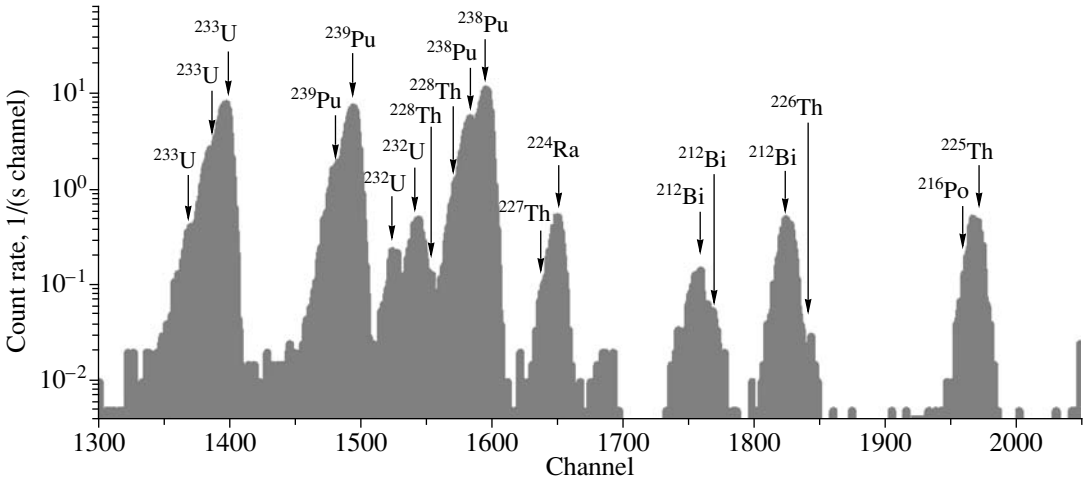

Fig. 1. Measured ^{233}U + ^{238}Pu + ^{239}Pu spectrum.

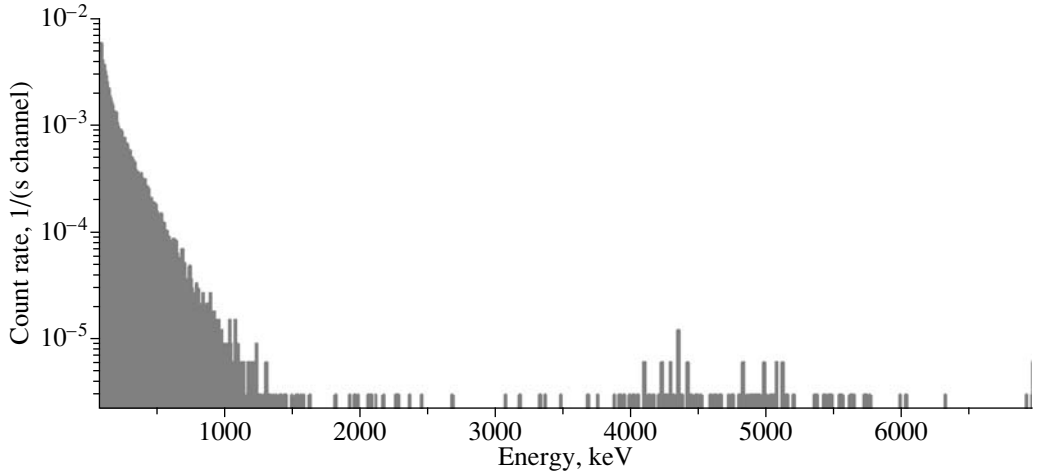

Fig. 2. Background count of the α spectrometer; the statistics collection time was 105 h.

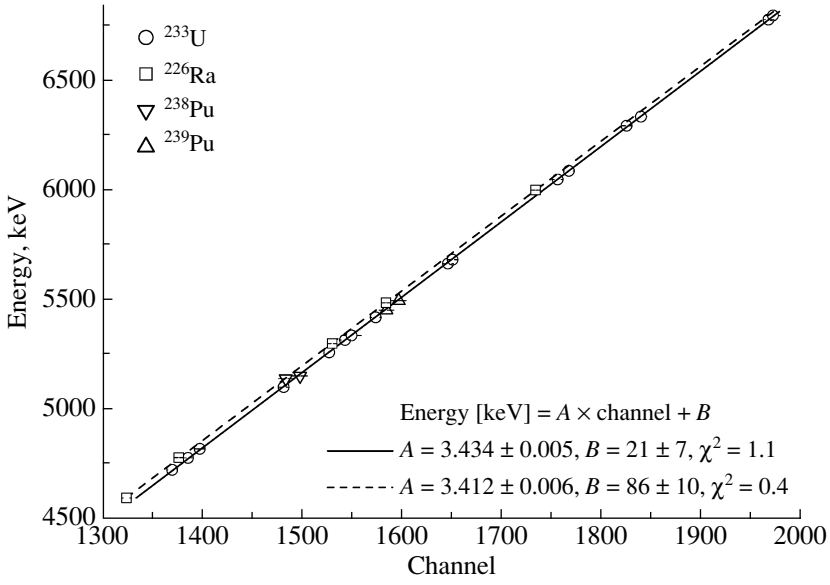

Fig. 3. Energy calibration curve of the α spectrometer.

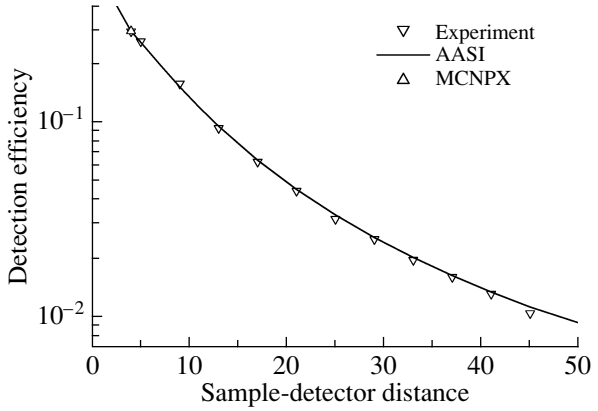

Fig. 4. Experimental (using ^{239}Pu) and calculated (AASI, MCNPX) detection efficiencies of the α spectrometer versus the distance between the sample and detector.

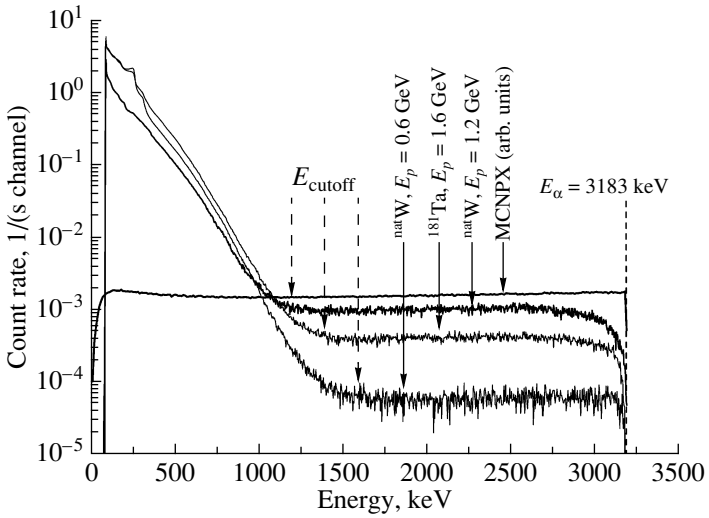

Fig. 5. Example of measured α spectra of irradiated $^{\text{nat}}$W and ^{181}Ta samples. Possible variants of $A(E)$ as the integral of the spectrum measured for energies from E_{cutoff} to 3183 keV are presented.

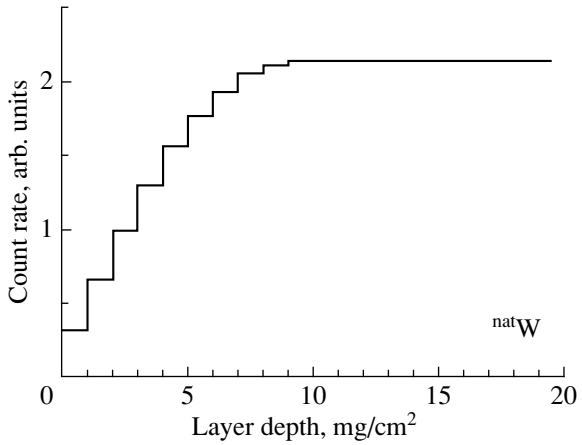

Fig. 6. Calculated count rate of the α detectors versus the thickness of the $^{\text{nat}}$W sample.

the excitation functions of appearing nuclei, as well as different irradiation durations and deexcitation times, is responsible for the absence of the constant energy bound of the β and α spectra.

The cross section for the production of ^{148}Gd is calculated by the formula

$$\sigma = \frac{\hat{R}^{\text{cum}}}{\hat{\Phi}}, \qquad (1)$$

where $\hat{R}^{\text{cum}}$ is the reaction rate of the production of ^{148}Gd and $\hat{\Phi}$ is the proton fluence.

Since the chemical separation of ^{148}Gd was not performed in view of a small amount of produced ^{148}Gd, it is impossible to directly determine the count rate of α particles in the peak. For this reason, the method for its determination was based on the calculation of the specific activity of ^{148}Gd in the sample.

The specific activity of ^{148}Gd in the ^{181}Ta and $^{\text{nat}}$W samples was determined by comparing the calculated and experimental α spectra, obtained in the identical geometries of the measurements, under the assumption that the count rate in a given energy range for samples with identical geometric shapes and sizes and a uniform distribution of ^{148}Gd is proportional to the specific activity of ^{148}Gd. The mean free paths of 3183-keV α particles in ^{181}Ta and $^{\text{nat}}$W are 9.88 and 10.09 mg/cm^2, respectively [7]. The calculated count rate for cylindrical samples in the chosen energy range of the α spectrum as a function of their thickness is shown in Figs. 6 and 7. It is seen that the thickness of the samples is much larger than the mean free path of α particles in these materials.

In this approach, it is necessary to take into account the following factors. As was mentioned above, the detector responds not only to α particles, but also to β radiation and characteristic γ radiation of radioactive nuclei appearing in the samples together with ^{148}Gd. Correspondingly, it is necessary to introduce the boundary energy E_{cutoff} in order to separate the region of the detection of the α peak free from β and γ components. To determine the boundary energy E_{cutoff}, we carried out additional experiments in which each sample was screened by a 15-μm aluminum foil. As an example, Fig. 8 shows the spectrum of $^{\text{nat}}W(E_p = 800$ MeV) with and without a foil (15-μm Al).

To simulate the spectrum of α particles from ^{148}Gd, we used the MCNPX code, which makes it possible to calculate the energy distribution of pulses $\tilde{A}(E)$ in the volume of the α detector taking into account all nuclear interactions of α particles with surroundings. In calculating $\tilde{A}(E)$, the total energy released in the volume of the Si detector in a single "calculated history" is taken into account.

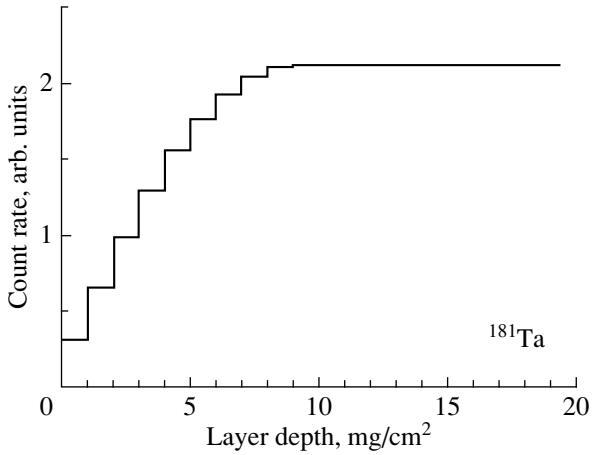

Fig. 7. As in Fig. 6, but for ^{181}Ta.

In accordance with the above consideration, the formula for the determination of the reaction rate of the production of ^{148}Gd has the form

$$R = \frac{1}{N_{\text{tag}}} \frac{A_{\text{cutoff}}}{\tilde{A}_{\text{cutoff}}} \frac{1}{1 - e^{-\lambda t_{\text{irr}}}}, \qquad (2)$$

where $\tilde{A}_{\text{cutoff}}$ is the count rate in the calculated spectrum in the energy range from E_{cutoff} to 3183 keV, A_{cutoff} is the count rate for the measured spectrum in the same energy range, t_{irr} is the sample irradiation time, and N_{tag} is the number of nuclei in the sample.

The resulting cross sections for the production of ^{148}Gd are summarized in Table 3, where the cross sections that were obtained in [4] for energies of 0.6 and 0.8 GeV and which are in agreement within the experimental errors with the data obtained in our study are also presented.

THEORETICAL SIMULATIONS

To determine the predictive power of modern intranuclear-cascade models, the measureD data for ^{148}Gd were compared with the results obtained with the MCNPX(BERTINI), MCNPX(ISABEL), CEM03.02, INCL4.2, INCL4.5, CASCADE.07, and PHITS codes widely used in various applications—in particular, in designing pilot versions of electronuclear facilities.

The interaction of protons with $^{\text{nat}}$W and ^{181}Ta was simulated for 18 proton energies from 0.3 to 3.5 GeV for each model. The cumulative yields of ^{148}Gd were calculated according to the scheme presented in Fig. 9. Among 47 parent nuclides presented in the scheme, 32 nuclides appear in the interaction of protons with $^{\text{nat}}$W and ^{181}Ta. Note that, owing to

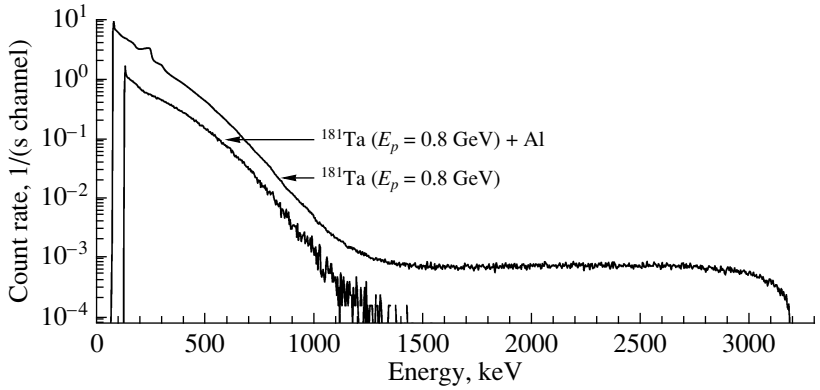

Fig. 8. Spectra of ^{nat}W ($E_p = 800$ MeV) with and without the decelerating screen (15-μm Al foil).

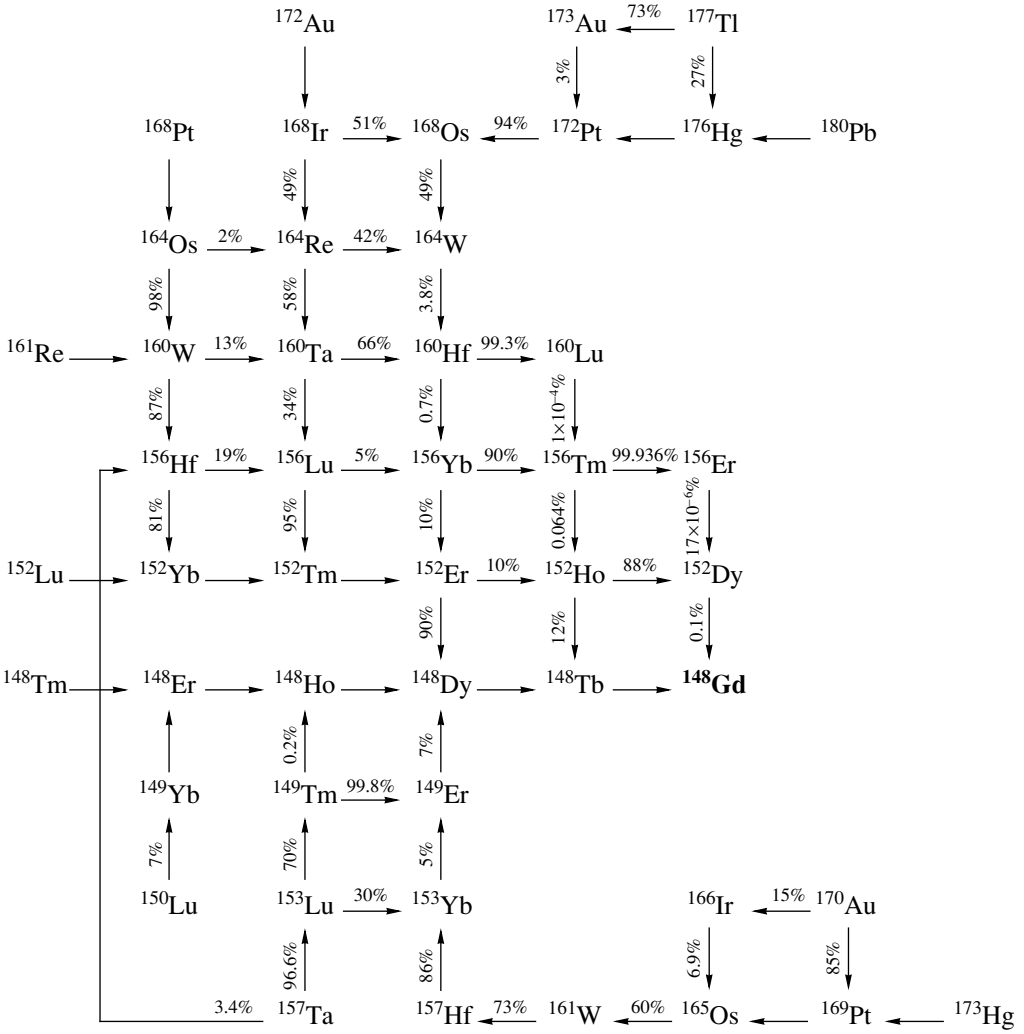

Fig. 9. Decay chains of the parents of ^{148}Gd.

α transitions in parents, the energy threshold of the cumulative yield of ^{148}Gd can be much lower than the threshold of the independent yield.

The resulting excitation functions were compared with those calculated with intranuclear cascade codes BERTINI, ISABEL, CEM03.02, INCL4.2, INCL4.5, CASCADE07, and PHITS [8–14]. The formulas for the convolution of the calculated inde-

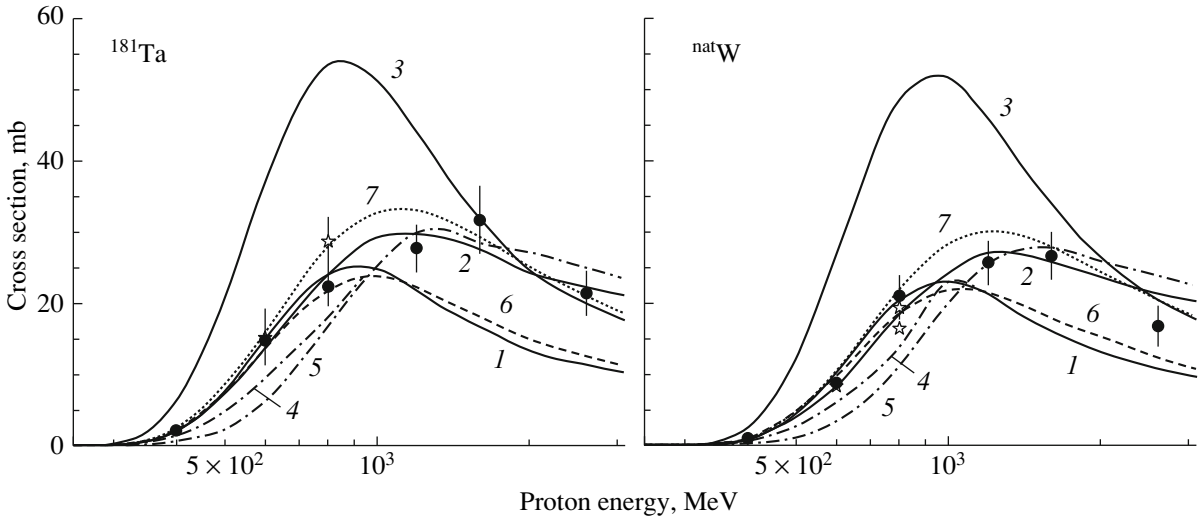

Fig. 10. Experimental and calculated excitation functions of the production of ^{148}Gd in ^{nat}W and ^{181}Ta. The experimental data are taken from (●) this work and (☆) [4]. Lines *1*, *2*, *3*, *4*, *5*, *6*, and *7* represent the BERTINI, INCL4.5, CEM03.02, ISABEL, INCL4.2, PHITS, and CASCADE07 calculations, respectively.

pendent cross sections into cumulative cross sections were given in [3, 15]. Examples of the calculated and experimental excitation functions are shown in Fig. 10.

CONCLUSIONS

The experimental and calculated excitation functions for the production of ^{148}Gd in ^{nat}W and ^{181}Ta are compared in Fig. 10 and in Table 3. One can see that the theoretical predictions based on all models, except for INCL4.5 and CASCADE07, only qualitatively describe the shape of the excitation functions. Therefore, no model can be recommended without a reference to experimental data.

ACKNOWLEDGMENTS

This work was supported by the International Science and Technology Center, project no. 3266, and by the State Nuclear Energy Corporation Rosatom.

REFERENCES

1. Yu. E. Titarenko, V. F. Batyaev, E. I. Karpikhin, et al., http://www-nds.iaea.org/reports/indc-ccp-434.pdf
2. Yu. E. Titarenko, O. V. Shvedov, V. F. Batyaev, et al., Phys. Rev. C **65**, 064610 (2002).
3. Yu. E. Titarenko, V. F. Batyaev, A. Yu. Titatenko, et al., Phys. Rev. C **78**, 034615 (2008).
4. K. C. Kelley, N. E. Hertel, E. J. Pitcher, et al., Nucl. Phys. A **760**, 225 (2005).
5. Yu. E. Titarenko, S. P. Borovlev, M. A. Butko, et al., Yad. Fiz. **74**, 531 (2011) [Phys. Atom. Nucl. **74**, 507 (2011)].
6. T. Siiskonen and R. Pollanen, Nucl. Instrum. Methods Phys. Res. A **550**, 425 (2005).
7. http://tvdg10.phy.bnl.gov/LETCalc.html
8. J. C. Hendricks et al., Report LA-UR-05-2675, LANL (2005); http://mcnp.lanl..gov/
9. S. G. Mashnik and A. J. Sierk, J. Nucl. Sci. Technol. Suppl. **2**, 720 (2002).
10. A. Boudard, J. Cugnon, S. Leray, and C. Volant, Phys. Rev. C **66**, 044615 (2002).
11. J. Cugnon, A. Boudard, S. Leray, et al., ISBN 978-92-0-150410-4, SM/SR-02 (2010).
12. A. R. Junghans et al., Nucl. Phys. A **629**, 635 (1998).
13. H. Iwase et al., J. Nucl. Sci. Technol. **39**, 1142 (2002); http://phits.jaea.go.jp/OvPhysicalModelsJQMD.html
14. H. Kumawat et al., Nucl. Instrum. Methods Phys. Res. B **266**, 604 (2008).
15. Yu. E. Titarenko, V. F. Batyaev, V. M. Zhivun, et al., INDC(CCP)-0447, IAEA (Oct. 2009); http://www-nds.iaea.org/reports-new/indc-reports/indc-ccp/

Translated by R. Tyapaev